

# Novel benzylidene cyclopentanone dyes for two-photon photopolymerization

Jianqiang Xue<sup>a,b</sup>, Yuxia Zhao<sup>a,\*</sup>, Jie Wu<sup>a,b</sup>, Feipeng Wu<sup>a,\*</sup>

<sup>a</sup> *Laboratory of Organic Optoelectronic Functional Materials and Molecular Engineering, Technical Institute of Physics and Chemistry, Chinese Academy of Sciences, Beijing 100080, PR China*

<sup>b</sup> *Graduate University of Chinese Academy of Sciences, Beijing, 100049, PR China*

Received 4 July 2007; received in revised form 27 September 2007; accepted 12 October 2007

Available online 22 October 2007

## Abstract

Two novel benzylidene cyclopentanone dyes (**1** and **2**) containing coumarin moiety were synthesized. Their photophysical properties were investigated using UV–vis spectra, fluorescence spectra and two-photon excited spectra. The maximum two-photon absorption cross-sections ( $\delta_{\max}$ ) of two compounds were determined as 939 GM and 1150 GM, respectively, with femtosecond laser pulses. Combined with commercial photoinitiator 4,4'-dimethyl-diphenyliodonium hexafluorophosphate (Omnicat 820), both of two dyes exhibited higher sensitizing photopolymerization efficiency than the common used high-efficient photosensitizer 2,5-bis-[4-(dimethylamino)-benzylidene]-cyclopentanone in one-photon photopolymerization experiments. Using **2** as sensitizer or initiator directly, 2D and 3D nanopatterns were successfully fabricated by two-photon initiated polymerization. © 2007 Elsevier B.V. All rights reserved.

**Keywords:** Photosensitizer; Benzylidene cyclopentanone; Coumarin; Two-photon absorption; Photopolymerization

## 1. Introduction

As a powerful tool for realizing high-density optical data storage [1] and three-dimensional micro-fabrication of functional devices [2,3], two-photon initiated polymerization (TPIP) has attracted much attention in recent years. Large amount of two-photon absorption (TPA) compounds have been reported [4–6]. However, seldom of them are available for TPIP due to their low photopolymerization sensitizing or initiating efficiency and high synthesis cost. Commercial available UV photoinitiators are still preferred by pioneer researchers on TPIP [7,8]. Though their TPA cross-section ( $\delta$ ) values are normally less than 40 GM [9]. Thus, it is a significant study to explore compounds with both large  $\delta$  value and high photopolymerization sensitizing or initiating quantum yield through simple synthesis process.

Benzylidene cyclopentanone dyes have been extensively investigated as high-efficient photosensitizers in common photopolymerization combined with commercial available photoinitiators, 4,4'-dimethyl-diphenyliodonium hexafluorophos-

phate (Omnicat 820) or *o*-Cl-hexaarylbisimidazole (HABI) [10,11]. In our previous study [12], we had reported that the  $\delta$  value of a typical benzylidene cyclopentanone dye, 2,5-bis-[4-(dimethylamino)-benzylidene]-cyclopentanone (**BDMA**), was 100–500 GM within 700–900 nm, which was comparatively high based on its low molecular weight and synthesis cost. Coumarin dyes are also high-efficient photosensitizers in photopolymerization [13,14]. They can match well with amine, hexaarylbisimidazole or iodonium salts to compose high-efficient photoinitiating systems. In addition, the  $\delta$  values of coumarin dyes could be enhanced efficiently through proper molecular designs [15,16].

In this letter, we synthesized two novel benzylidene cyclopentanone dyes incorporating coumarin moiety through a simple route, studied their photophysical and photochemical properties, and tested their application in two-photon photopolymerization. Some interesting results are expected by such a combination.

## 2. Experimental

2,5-Bis-[4-(dimethylamino)-benzylidene]-cyclopentanone (**BDMA**) and 2-[4-(dimethylamino)-benzylidene]-cyclopentanone (**DMA**) were prepared according to the literature [17]. 4,

\* Corresponding authors. Tel.: +86 10 82543571; fax: +86 10 82543491.  
E-mail addresses: [yuxia.zhao@mail.ipc.ac.cn](mailto:yuxia.zhao@mail.ipc.ac.cn) (Y. Zhao),  
[fpwu@mail.ipc.ac.cn](mailto:fpwu@mail.ipc.ac.cn) (F. Wu).

4'-Dimethyl-diphenyliodonium hexafluorophosphate (Omnicat 820) was from TH-UNIS Insight Co. Ltd. 4-(*N,N*-diethylamino) salicyl (used after recrystallization) was obtained from Tianjin De'ai Co. Ltd. *o*-Cl-hexaarylbisimidazole (HABI) was from Tokyo Kasei Kogyo Co. Ltd. 3-Mercapto-4-methyl-1,2,4-triazole (MMT) was from Avocado. 2-Phenoxyethyl acrylate (SR339), pentaerythritol triacrylate (SR444) and epoxy acrylate (CN124A80) were from Sartomer Co. Ltd., and used as received. Diethyl malonate, Rhodamine B and other A.R. grade reagents were all from Beijing Beihua Co. Ltd., and used after purification by common methods.

UV-vis absorption spectra were measured on a Jasco V-530 spectrophotometer. One-photon fluorescence spectra were performed on a Hitachi F-4500 fluorescence spectrophotometer. FTIR spectra were monitored on a Nicolet 5700 infrared spectrophotometer.  $^1\text{H}$  NMR spectra were obtained on a Bruker DPX400 spectrometer. Mass spectra were carried out on Bruker APEX-2.

### 2.1. 7-Diethylamino-coumarin (DEAC)

4-Diethylamino-salicylal (0.2 mol, 38.6 g) and diethyl malonate (0.22 mol, 35.2 g) were mixed and refluxed in 60 ml of ethanol together with 2 ml of pyridine and 0.23 ml of acetic acid as catalyst for 8 h. After distilled to remove volatile compositions, 40 ml hydrochloric acid was added drop wise to acidify the mushy under fierce stirring and reflux. After 10 h, the suspension was cooled and white precipitation was collected. Then, it was neutralized by dilute NaOH solution to give the pale yellow product DEAC. The crude product was recrystallized by ethanol to give a total yield of 52% m.p. 88–89 °C [literature [18] m.p. 90–94 °C].

### 2.2. 7-(Diethylamino)-3-formylcoumarin (DEAFC)

Using DEAC as reactive material, DEAFC was prepared and purified following the normal procedure of Vilsmeier reaction according to the literature [19] and characterized by  $^1\text{H}$  NMR [26].

### 2.3. Compound 1

DEAFC (2 mmol, 0.49 g) and DMA (2 mmol, 0.43 g) were dissolved in 8 ml of ethanol and 0.8 ml of xylene together with 0.06 g NaOH. After 6 h of refluxing, cooled, the red precipitation was collected and washed with ethanol. The crude product was purified by column chromatography on silica gel ( $V_{\text{CH}_2\text{Cl}_2}:V_{\text{AcOEt}} = 100:3$ ), yield 43% and characterized by  $^1\text{H}$  NMR and HRMS [26].

### 2.4. Compound 2

The mixture of DEAFC (2 mmol, 0.49 g) and cyclopentanone (1 mmol, 0.084 g) were dissolved in 10 ml of ethanol and 1.6 ml of xylene together with 0.08 g NaOH. After 8 h of refluxing, cooled, bright red precipitation was collected and washed with

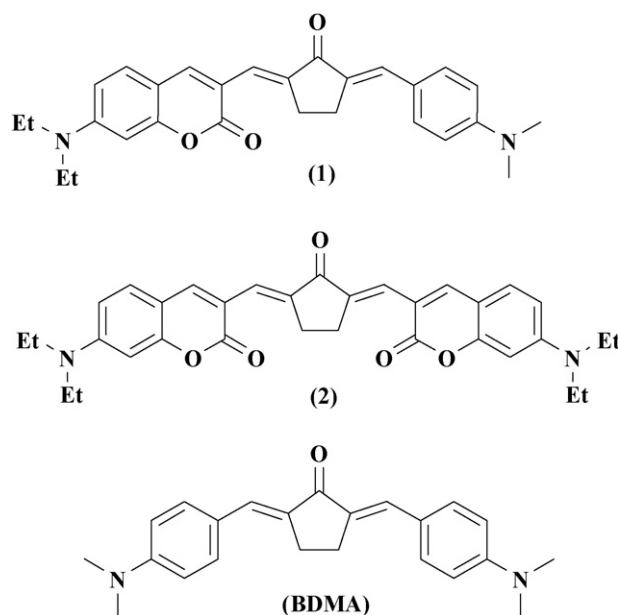


Fig. 1. Chemical structures of **1**, **2** and **BDMA**.

ethanol. The crude product was purified by column chromatography on silica gel ( $V_{\text{CH}_2\text{Cl}_2}:V_{\text{AcOEt}} = 100:5$ ), yield 40% and characterized by  $^1\text{H}$  NMR and HRMS [26].

The chemical structures of **1**, **2** and **BDMA** are shown in Fig. 1.

Solvatochromism effects of compounds were performed in a series of mixed solvents of acetonitrile and toluene with a concentration of  $10^{-5}$  M and  $10^{-6}$  M for UV-vis spectra and fluorescence spectra, respectively. The polarity of solvent was represented by the solvent polarity function ( $\Delta f$ ) which was calculated from solvent's refractive index and dielectric constant [20,21]. The fluorescence quantum yields of **1**, **2** and **BDMA** in chloroform were determined by using Rhodamine B as a standard and refractive index correction was performed [22].

TPA cross-section ( $\delta$ ) values of compounds in chloroform solution ( $2 \times 10^{-4}$  M) were determined using the two-photon-excited fluorescence (TPEF) technique with femtosecond laser pulses following the experimental protocol described in detail by Xu and Webb [23]. The excitation light sources were a mode-locked Tsunami Ti:sapphire laser (720–880 nm, 80 MHz, <130 fs) and OPA-800CF plus SHG (840–1100 nm, 1000 Hz, <200 fs). Rhodamine B in methanol solution ( $10^{-4}$  M) was used as reference. To avoid any contribution from other photophysical/photochemical processes, the intensity of input pulses were adjusted to a proper regime to ensure a quadratic dependence of the fluorescence intensity vs. excitation pulse energy.  $\delta$  was calculated by the following equation [23]:

$$\delta = \frac{S_s \Phi_r \varphi_r c_r}{S_r \Phi_s \varphi_s c_s} \delta_r$$

Here subscription r and s stands for the reference and sample, respectively;  $S$  the integral area of the two-photon-excited fluorescence;  $\Phi$  the quantum yield;  $\varphi$  the overall fluorescence collection efficiency of the experimental apparatus; and  $c$  is the number density of the molecules in solution.

Table 1  
One- and two-photon optical properties of **1**, **2** and **BDMA** in chloroform

Compound	$\lambda_{\max}^a$ (nm)	$\epsilon_{\max}^a$ ( $10^4 \text{ M}^{-1} \text{ cm}^{-1}$ )	$\lambda_{\max}^{\text{fl}}$ (nm)	$\Delta v_{\text{ss}}^b$ ( $10^3 \text{ cm}^{-1}$ )	$\Phi^c$	$\delta_{\max}$ (GM)	$\delta_{\text{avg}}$ (GM)	$\delta_{780 \text{ nm}}$
<b>1</b>	500.0	6.6	564.0	2.27	0.09	939	269	243
<b>2</b>	521.0	8.9	580.0	1.95	0.15	1150	334	390
<b>BDMA</b>	466.5	6.5	535.0	2.75	0.13	526	201	248

<sup>a</sup>  $\epsilon_{\max}$  is molar absorption coefficient.

<sup>b</sup>  $\Delta v_{\text{ss}}$  is Stoke's shifts.

<sup>c</sup>  $\Phi$  is fluorescence quantum yield.

In one-photon photopolymerization experiments, monomers were a mixed acrylate of SR339, SR444 and CN124A80 ( $m_{\text{SR339}}:m_{\text{SR444}}:m_{\text{CN124A80}} = 1:3:5$ ). Coinitiator was Omnicat 820. Compounds **1**, **2** and **BDMA** were used as sensitizer, respectively. A small amount of dichloromethane and methanol ( $m:m = 9:1$ ) was used as solvent. The mixed photocurable solutions were poured into glass cells with a thickness of 0.5 mm. The light source was an EFOS Lite 50 W miniature arc lamp with a 5 mm crystal optical fiber. Its intensity of irradiation was  $20 \text{ mW/cm}^2$ . A band-pass filter was inserted to choose light between 400–500 nm for our experiments. The polymerization conversion efficiency was calculated by the change of the double bond absorption peak area centered at  $6164 \text{ cm}^{-1}$  in near-IR region.

The same mixed monomers were used in two-photon photopolymerization experiments with **2** as sensitizer, HABI and MMT as coinitiator. The laser (Tsunami Ti:sapphire, 780 nm, 80 MHz, 80 fs) was tightly focused via an oil-immersion objective lens ( $100\times$ ,  $\text{NA} = 1.4$ , Olympus) into the sample which was fixed on a  $xyz$ -step motorized stage controlled by a computer. After laser fabrication, the unpolymerized resin was washed out using acetone. The obtained microstructures were characterized by SEM (Hitachi S-4300FEGd).

### 3. Results and discussion

#### 3.1. UV-vis absorption and steady-state fluorescence

Optical properties of compounds in chloroform and mixed solvents of toluene/acetonitrile with different polarity are listed in Tables 1 and 2. It is shown that with increasing solvent polarity the absorption peaks and fluorescence emission peaks of three compounds all shift to longer wavelengths. In addition,

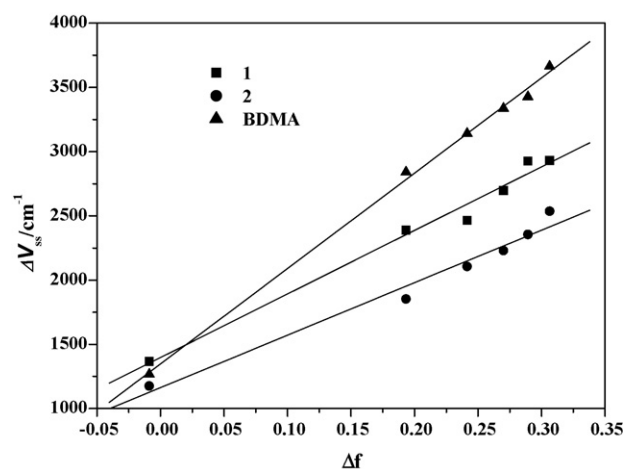


Fig. 2. Stoke's shift of dyes vs. the solvent polarity parameter  $\Delta f$ .

the red shifts in fluorescence spectra are much larger than those in absorption spectra for three dyes, which indicate that their absorption bands all have charge-transfer character and their excited-state possess higher polarity than their ground-state. The solvatochromism effect can be explained by Lippert–Mataga equation [20,21]. The good linear relationship of Stokes shift vs. solvent polarity parameter  $\Delta f$  is shown in Fig. 2. And the large slope values confirm that all three dyes have large intramolecular charge-transfer (ICT) from ground-state to excited-state.

In chloroform, the absorption peak of **1** and **2** exhibits a large red-shift as 33.5 and 54.5 nm, respectively, compared to **BDMA**. It might be due to the increased length of conjugation structure of coumarin moiety. On the other hand, **BDMA** shows the biggest Stoke's shift and **2** shows the smallest, which might be due to charge localization by the rigid coumarin moiety decreasing the

Table 2  
Linear optical properties of **1** and **2** in mixed solvents

Solvent (%)	<b>1</b>				<b>2</b>				<b>BDMA</b>			
	$\lambda_{\max}^a$ (nm)	$\lambda_{\max}^{\text{fl}}$ (nm)	$\epsilon_{\max}^a$	$\Delta v_{\text{ss}}^b$	$\lambda_{\max}^a$ (nm)	$\lambda_{\max}^{\text{fl}}$ (nm)	$\epsilon_{\max}^a$	$\Delta v_{\text{ss}}^b$	$\lambda_{\max}^a$ (nm)	$\lambda_{\max}^{\text{fl}}$ (nm)	$\epsilon_{\max}^a$	$\Delta v_{\text{ss}}^b$
0 <sup>c</sup>	485.5	520.0	6.32	1.37	500.0	531.2	5.85	1.17	452.5	480.0	7.23	1.27
20	495.5	562.0	7.47	2.39	519.0	574.2	7.86	1.85	460.5	529.8	7.29	2.84
40	497.5	567.0	8.10	2.46	521.0	585.2	6.24	2.11	463.0	541.8	7.37	3.14
60	497.5	574.6	8.50	2.70	522.5	591.4	6.17	2.23	462.0	546.2	7.39	3.34
80	497.0	581.6	8.64	2.93	522.5	595.8	6.22	2.35	461.5	548.2	7.91	3.43
100	495.0	579.0	8.85	2.93	520.0	599.0	8.41	2.54	459.0	551.8	8.46	3.66

<sup>a</sup> The unit is  $10^4 \text{ M}^{-1} \text{ cm}^{-1}$ .

<sup>b</sup> The unit is  $10^3 \text{ cm}^{-1}$ .

<sup>c</sup> The numbers in the sheet denote the volume percentage of acetonitrile in toluene.

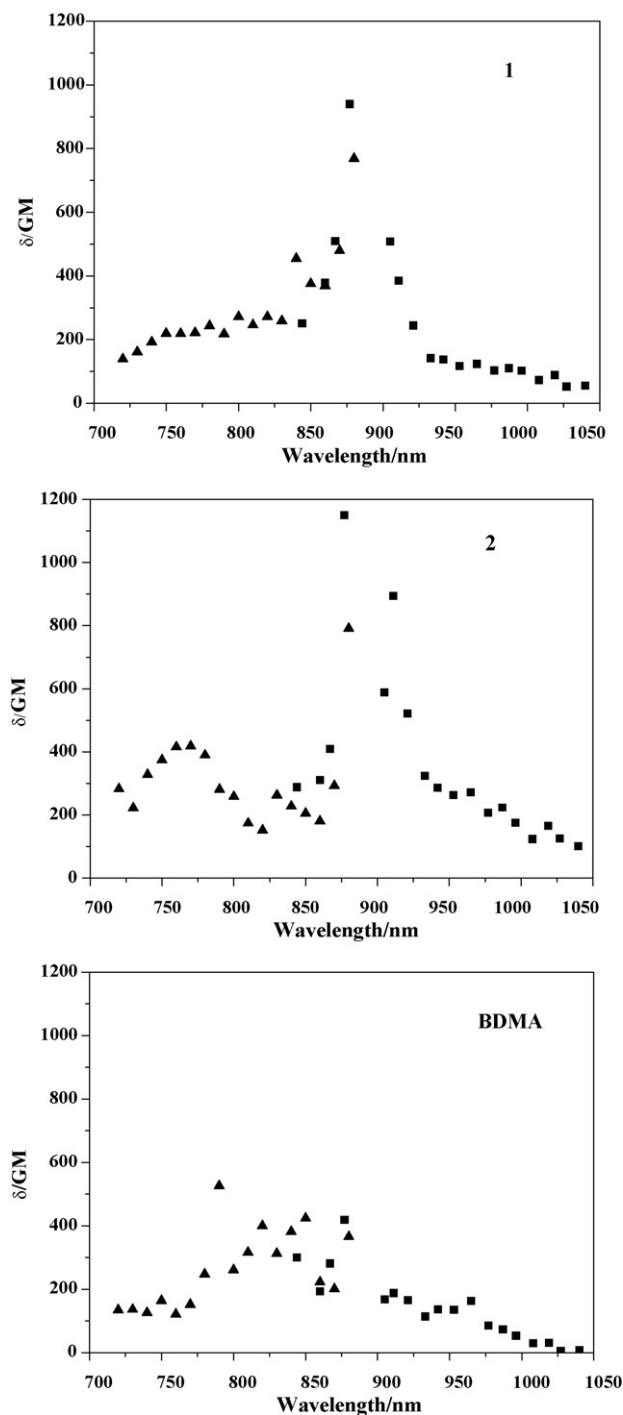


Fig. 3. Two-photon excitation spectra of dyes **1**, **2** and **BDMA**, [dye] =  $2 \times 10^{-4}$  M, in chloroform. The excited source are Tsunami (filled triangle) and OPA (filled square), respectively.

ICT of the whole molecular. The fluorescence quantum yields of **1**, **2** and **BDMA** are as low as 0.09, 0.15 and 0.13, respectively, indicating they can be used as good triplet sensitizers in photopolymerization.

### 3.2. TPA cross-sections

The two-photon excitation (TPE) spectra were measured over a broad range of 720–1050 nm.  $\delta$  values of three compounds

were calculated and shown in Fig. 3. It is shown that the data get from different excited sources are coincident to each other within their overlapped area. The discrepancy might be due to different peak power, pulse width and frequency between Tsunami and OPA plus SHG. The TPE peak wavelengths ( $\delta_{\max}$ ) of **1** and **2** appear at 877 nm, have a blue-shift about 150 nm compared to the double wavelength of their linear absorption peaks. This suggests that some higher excited singlet states are reached with greater probability by TPE than by one-photon excitation. A small peak can be observed around the region 770 nm, especially for **2**. It might correspond to TPA of the ICT of coumarin moiety.

Within the whole measured range **1** and **2** show stronger TPA than **BDMA**. The  $\delta_{\max}$  of **1** and **2** are 939 GM and 1150 GM, respectively, while the  $\delta_{\max}$  of **BDMA** is 526 GM. The average TPA cross-section ( $\delta_{\text{avg}}$ ) of three compounds also have an order of  $2 > 1 > \text{BDMA}$ . It indicates that to incorporate coumarin moiety can efficiently increase the TPA capabilities of benzylidene cyclopentanone dyes.

### 3.3. One-photon photopolymerization

The sensitizing efficiencies of dyes to the common used coinitiator Omniscat 820 were investigated by one-photon pho-

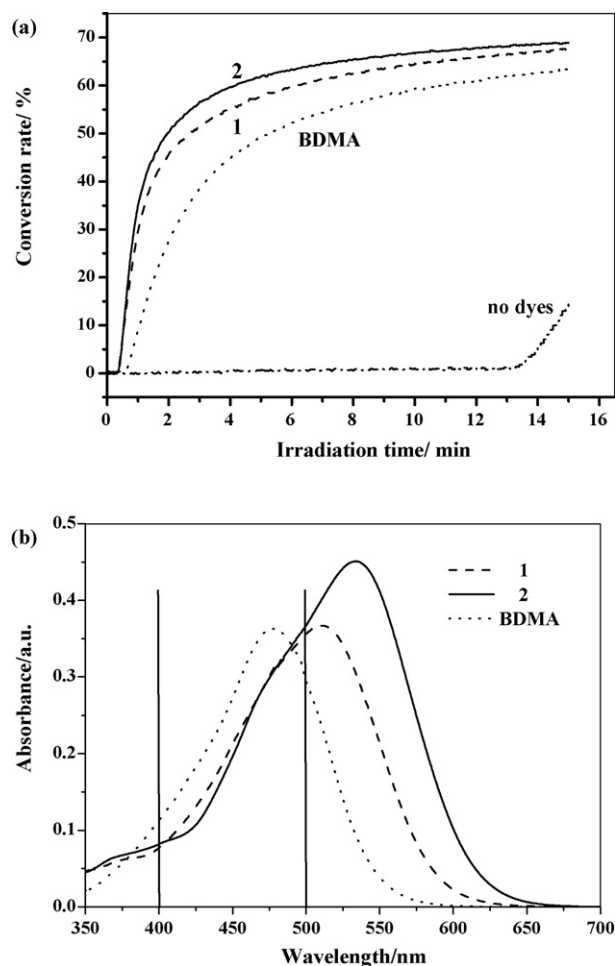


Fig. 4. (a) Double-bond conversion rate vs. irradiation time and (b) absorption spectra of resin films.



Table 3  
Components of photocurable resins used in TPIP

Resin	Monomer (wt%)	Dye 2 (wt%)	HABI (wt%)	MMT (wt%)	$E_{th}^a$ (mW)	$E_{break}^b$ (mW)	DPR <sup>c</sup>
R <sub>1</sub>	100	0	0	0	2.84	3.39	1.19
R <sub>2</sub>	99.99	0.01	0	0	2.11	3.39	1.61
R <sub>3</sub>	99.9	0.1	0	0	1.05	3.39	3.29
R <sub>4</sub>	97.99	0.01	1	1	1.02	3.39	3.32
R <sub>5</sub>	97.9	0.1	1	1	0.44	3.39	7.7

<sup>a</sup> TPIP threshold energy.

<sup>b</sup> Laser-induced breakdown threshold energy.

<sup>c</sup> Dynamic power range of resins.

topolymerization. Through monitoring the relative change of the double bond absorption of acrylate monomers at  $6164\text{ cm}^{-1}$  in near-IR region, the sensitizing efficiencies of different dyes were determined. The double bond conversion rate vs. time curves of photocurable resin films containing different dyes are displayed in Fig. 4a. For comparison, a resin film with only Omnical 820 was also tested under same experimental conditions. The results show that all photosensitizers have a significant benefit on the efficiency of the polymerization reaction. In addition, the photosensitizing efficiencies of three dyes have an order of  $2 > 1 > \text{BDMA}$ . In UV–vis spectra of photocurable resin films (Fig. 4b), it is shown that within 400–500 nm the absorption area of **BDMA** is larger than those of **1** and **2**. Thus, the highest photosensitizing efficiency of **2** means it has higher photosensitizing quantum yield than **1**, which in turn is higher than **BDMA**.

#### 3.4. Two-photon initiated polymerization

Because compound **2** exhibits the largest  $\delta$  and the highest photosensitizing efficiency among three dyes, we choose **2** as

sensitizer to carry out TPIP experiments. For comparison, five resins (R<sub>1</sub>–R<sub>5</sub>) with different components (listed in Table 3) were investigated. R<sub>1</sub> was pure mixed monomers. R<sub>2</sub> contained 0.01% (wt%) **2** as initiator. R<sub>3</sub> contained 0.1% **2**. R<sub>4</sub> contained 0.01% **2**, 1% HABI and 1% MMT as coinitiator. R<sub>5</sub> contained 0.1% **2**, 1% HABI and 1% MMT. Using line scan method [24], the TPIP threshold energy ( $E_{th}$ ) and the laser-induced breakdown threshold energy ( $E_{break}$ ) of R<sub>1</sub>–R<sub>5</sub> were determined. Here,  $E_{th}$  was defined by the lowest laser power at focus point that can guarantee fabricating a solid line with a line scan speed of  $10\ \mu\text{m/s}$ ,  $E_{break}$  was defined by the lowest laser power at focus point that can induce intense damage in materials under the same scan speed, which could be observed by CCD on live.

The experimental results are listed in Table 3. Compared to R<sub>1</sub>, the  $E_{th}$  of R<sub>2</sub> and R<sub>3</sub> decrease to 2.11 mW and 1.05 mW for containing 0.01% and 0.1% dye **2** as photoinitiator, respectively, which proves dye **2** is a high-efficient TPIP photoinitiator. Furthermore, after added 1% HABI and 1% MMT as coinitiator, the  $E_{th}$  of R<sub>4</sub> and R<sub>5</sub> decrease to 1.02 mW and 0.44 mW compared to 2.11 mW of R<sub>2</sub> and 1.05 mW of R<sub>3</sub>, respectively,

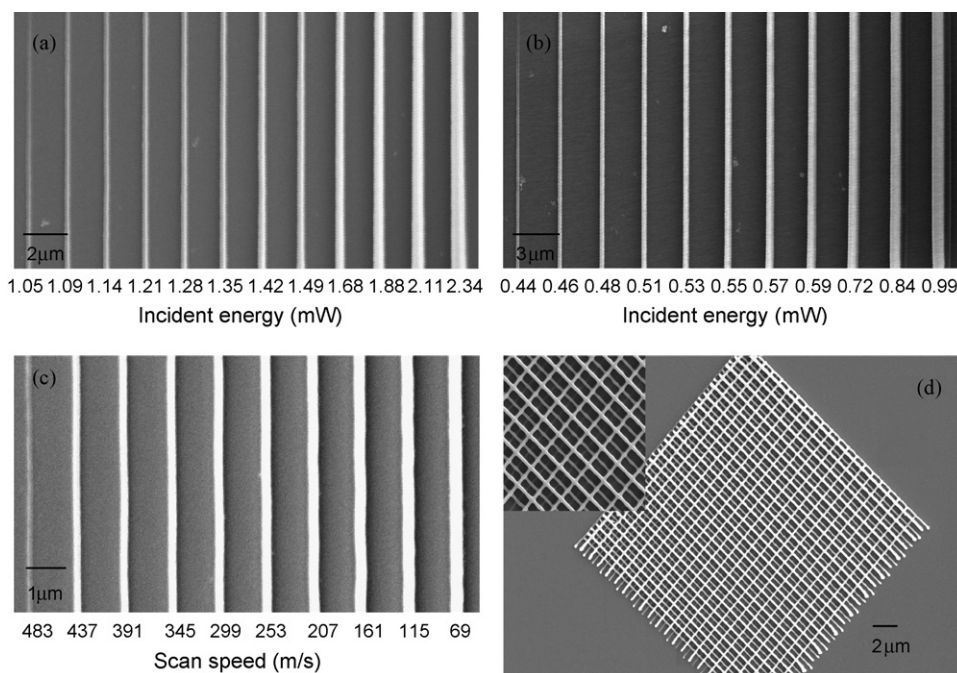


Fig. 5. 2D nanopattern fabricated in R<sub>3</sub> (a) and R<sub>5</sub>; (b) by changing the incident energy with a fixed line scan speed of  $10\ \mu\text{m/s}$ , and in R<sub>4</sub>; (c) by adjusting the line scan speed with fixed incident energy of 1.6 mW; and (d) 3D wood pile structure fabricated in R<sub>3</sub> with 1.1 mW power and  $44\ \mu\text{m/s}$  scan speed.

which shows to add commercial UV components is an effective way to further decrease  $E_{th}$  of resins. Five resins exhibit same  $E_{break}$  as 3.39 mW. This should be due to their main part are same mixed monomers. We calculate the dynamic power range (DPR) of resins, which is defined as the ratio of  $E_{break}$  to  $E_{th}$  [3]. Obviously, lower  $E_{th}$  means higher DPR, leaving bigger room for power tuning in application.

An interesting phenomenon is noticed that polymerization of pure mixed monomers  $R_1$  can happen under 2.84 mW irradiation. We carefully repeated the experiment several times and confirmed this result. As we know it is the first time to report photopolymerization of pure acrylate monomers under a 780 nm femtosecond laser irradiation. Its very small DPR may be a reason why other researchers miss it. Because the absorption of  $R_1$  is cut off at 350 nm, this polymerization cannot be due to TPIP. We think the electron generation by avalanche ionization and the thermal effect accumulated under strong irradiance intensity with high-frequency proposed by Seet et al. [25] should be the real mechanism of this polymerization. For  $R_2$ – $R_5$ , under incident energy near to their  $E_{break}$  the avalanche ionization and thermal effect will prevail, but TPIP's contribution will increase sharply following the decrease of incident energy and become dominant under incident energy near to their  $E_{th}$  as Xing et al. reported [24].

2D nanopatterns were fabricated in resins by changing the incident energy with a fixed line scan speed or adjusting the line scan speed with fixed incident energy. It is shown (Fig. 5a–c) that line scan speed (which is related to exposure time) and incident energy both have significant effects on the line width. The highest resolution of 142 nm was obtained in this work. A 3D woodpile with 184 nm line width (Fig. 5d) was fabricated using  $R_3$  with 1.1 mW energy and 44  $\mu\text{m/s}$  scan speed. It indicates that **2** can be used as not only a high-efficient photosensitizer but also a high-efficient photoinitiator directly in TPIP.

#### 4. Conclusion

Two novel TPA dyes (**1** and **2**) incorporating coumarin moiety and benzylidene cyclopentanone moiety together were synthesized by a simple route. Compared to the common used high-efficient photosensitizer **BDMA**, The two-photon absorption capability and photosensitizing quantum yield of **1** and **2** were both enhanced. Compound **2** containing two coumarin moieties showed the largest  $\delta$  value as 1150 GM and the highest photosensitizing efficiency. Using **2** as sensitizer or initiator directly, 2D and 3D nanopatterns were successfully fabricated by TPIP. The results indicate that the introduction of coumarin moiety into benzylidene cyclopentanone dyes is a useful strategy to explore compounds with both large TPA and high photosensitizing efficiencies. Such compounds would have extensive application prospects in three-dimensional micro-fabrication and high-density optical data storage.

This work was supported by the National Science Foundation of China (Nos. 50403030 and 60477004). The authors thank Ms.

X. Fang for her help on TPEF measurement, thank Prof. J. Nie and Dr. Y. He for their help in RT-FTIR facilities, and thank Prof. X. Duan and Ms. X. Dong for their help on TPIP.

#### References

- [1] D.A. Parthenopoulos, P.M. Rentzepis, *Science* 245 (1989) 843–845.
- [2] B.H. Cumpston, S.P. Ananthavel, S. Barlow, D.L. Dyer, J.E. Ehrlich, L.L. Erskine, A.A. Heikal, S.M. Kuebler, I.-Y.S. Lee, D. McCord-Maughon, J.-Q. Qin, H. Rockel, M. Rumi, X.-L. Wu, S.R. Marder, J.W. Perry, *Nature* 398 (1999) 51–54.
- [3] H.-B. Sun, S. Kawata, *Adv. Polym. Sci.* 170 (2004) 169–273.
- [4] M. Albota, D. Beljonne, J.-L. Brédas, J.E. Ehrlich, J.-Y. Fu, A.A. Heikal, S.E. Hess, T. Kogej, M.D. Levin, S.R. Marder, D. McCord-Maughon, J.W. Perry, H. Röckel, M. Rumi, G. Subramaniam, W.W. Webb, X.-Li. Wu, C. Xu, *Science* 281 (1998) 1653–1656.
- [5] S.-J. Chung, K.-S. Kim, T.-C. Lin, G.S. He, J. Swiatkiewicz, P.N. Prasad, *J. Phys. Chem. B* 103 (1999) 10741–10745.
- [6] K.D. Belfield, A.R. Morales, J.M. Hales, D.J. Hagan, E.W. Van Stryland, V.M. Chapela, J. Percino, *Chem. Mater.* 16 (2004) 2267–2273.
- [7] S. Kawata, H.-B. Sun, T. Tanaka, K. Takada, *Nature* 412 (2001) 697–698.
- [8] L.H. Nguyen, M. Straub, M. Gu, *Adv. Funct. Mater.* 15 (2005) 209–216.
- [9] K.J. Schafer, J.M. Hales, M. Balu, K.D. Belfield, E.W. Van Stryland, D.J. Hagan, *J. Photochem. Photobiol. A: Chem.* 162 (2004) 497–502.
- [10] B.M. Monroe, W.K. Smothers, D.E. Keys, R.R. Krebs, D.J. Mickish, A.F. Harrington, S.R. Schicken, M.K. Armstrong, D.M.T. Chan, C.I. Weathers, *J. Imag. Sci.* 35 (1991) 19–25.
- [11] E.-J. Wang, J. Li, Y.-Y. Yang, *J. Photopolym. Sci. Technol.* 4 (1991) 157–164.
- [12] J. Wu, Y.-X. Zhao, X. Li, M.-Q. Shi, F.-P. Wu, X.-Y. Fang, *N. J. Chem.* 30 (2006) 1098–1103.
- [13] D.P. Specht, P.A. Martic, S. Farid, *Tetrahedron* 38 (1982) 1203–1211.
- [14] Q.-Q. Zhu, W. Schnabel, *Polymer* 37 (1996) 4129–4133.
- [15] Y.-X. Zhao, X. Li, F.-P. Wu, X.-Y. Fang, *J. Photochem. Photobiol. A: Chem.* 177 (2006) 12–16.
- [16] X. Li, Y.-X. Zhao, J. Wu, M.-Q. Shi, F.-P. Wu, *J. Photochem. Photobiol. A: Chem.* 190 (2007) 22–28.
- [17] T. Wang, F.-P. Wu, M.-Q. Shi, *Chem. Res. Chin. Univ.* 19 (2003) 470–473.
- [18] Q.-Y. Wu, E.V. Anslyn, *J. Mater. Chem.* 15 (2005) 2815–2819.
- [19] H. Takechi, Y. Oda, N. Nishizono, K. Oda, M. Machida, *Chem. Pharm. Bull.* 48 (2000) 1702–1710.
- [20] V.E. Lippert, *Z. Naturforsch.* 10a (1955) 541–545.
- [21] N. Mataga, Y. Kaifu, M. Koizumi, *Bull. Chem. Soc. Jpn.* 28 (1955) 690–691.
- [22] J.N. Demas, G.A. Crosby, *J. Phys. Chem.* 75 (1971) 991–1024.
- [23] C. Xu, W.W. Webb, *J. Opt. Soc. Am. B* 13 (1996) 481–491.
- [24] J.-F. Xing, X.-Z. Dong, W.-Q. Chen, X.-M. Duan, N. Takeyasu, T. Tanaka, S. Kawata, *Appl. Phys. Lett.* 90 (2007) 131106.
- [25] K.K. Seet, S. Juodkazis, V. Jarutis, H. Misawa, *Appl. Phys. Lett.* 89 (2006) 024106.
- [26] DEAF:  $^1\text{H}$  NMR (400 MHz,  $\text{CDCl}_3$ )  $\delta$ : 1.26 (t,  $J$  7.1 Hz, 6H), 3.47 (q,  $J$  7.1 Hz, 4H), 6.50 (d,  $J$  2.3 Hz, 1H), 6.64 (dd,  $J_1$  2.3 Hz,  $J_2$  9.0 Hz, 1H), 7.42 (d,  $J$  9.0 Hz, 1H), 8.26 (s, 1H), 10.14 (s, 1H). Compound **1**:  $^1\text{H}$  NMR (400 MHz,  $\text{CDCl}_3$ )  $\delta$ : 1.23 (t,  $J$  7.1 Hz, 6H), 3.04 (s, 6H), 3.06 (s, 4H), 3.44 (q,  $J$  7.1 Hz, 4H), 6.48 (d,  $J$  2.4 Hz, 1H), 6.60 (dd,  $J_1$  8.9 Hz,  $J_2$  2.4 Hz, 1H), 6.74 (d,  $J$  8.6 Hz, 2H), 7.30 (d,  $J$  8.9 Hz, 1H), 7.52 (d,  $J$  8.9 Hz, 2H), 7.55 (s, 1H), 7.73 (s, 1H), 7.78 (s, 1H). HRMS (FAB): Anal. Calcd. For  $\text{C}_{28}\text{H}_{30}\text{N}_2\text{O}_3$ : 442.2250. Found: 442.2248. Compound **2**:  $^1\text{H}$  NMR (400 MHz,  $\text{CDCl}_3$ )  $\delta$ : 1.23 (t,  $J$  7.1 Hz, 12H), 3.03 (s, 4H), 3.44 (q,  $J$  7.1 Hz, 8H), 6.45 (d,  $J$  2.1 Hz, 2H), 6.60 (dd,  $J_1$  8.8 Hz,  $J_2$  2.2 Hz, 2H), 7.31 (d,  $J$  8.8 Hz, 2H), 7.71 (s, 2H), 7.76 (s, 2H). HRMS (FAB): Anal. Calcd. For  $\text{C}_{33}\text{H}_{34}\text{N}_2\text{O}_5$ : 538.2475. Found: 538.2480.